



Cite this: *RSC Adv.*, 2021, **11**, 29925

Effects of aluminum chloride and coenzyme Q10 on the molecular structure of lipids and the morphology of the brain hippocampus cells

Abdu Saeed, ^{a,b} Safaa Y. Qusti,^c Rawan Hamdan Almarwani,^c Ebtihaj J. Jambi,^{cd} Eida M. Alshammari,^e Naeem F. Gusty^f and Maha J. Balgoon^c

Aluminum chloride (AlCl_3) is a neurotoxic substance, while coenzyme Q10 (CoQ10) is considered a lipid antioxidant. Herein, their effects on the molecular structure of lipids and the morphology of the hippocampus brain tissue were investigated. Three groups of Wistar albino male rats were used in this study. For four weeks, one group was kept as a control group; the second group was given AlCl_3 ; the third group was given AlCl_3 /CoQ10. Fourier transform infrared (FTIR) and histopathological examinations were utilized to estimate alterations in the molecular structure of the lipids and the cell morphology, respectively. The FTIR spectra revealed considerable decreases in the CH contents and alterations in the molecular ratios of $\text{olefinic}=\text{CH}/\nu_{\text{as}}(\text{CH}_3)$, $\nu_{\text{as}}(\text{CH}_2)/\nu_{\text{as}}(\text{CH}_3)$, and $\nu_{\text{as}}(\text{CH}_2)/[\nu_{\text{as}}(\text{CH}_2) + \nu_{\text{s}}(\text{CH}_2)]$ in the group given AlCl_3 . However, no significant changes were detected in those rats given AlCl_3 /CoQ10. Histopathology images uncovered shrinking and dark centers in the pyramidal cells of brain tissue hippocampal cells. The diameters of the pyramidal cells were estimated to be $4.81 \pm 0.55 \mu\text{m}$, $4.04 \pm 0.71 \mu\text{m}$, and $4.63 \pm 0.71 \mu\text{m}$ for the control, AlCl_3 , and AlCl_3 /CoQ10 groups, respectively. The study showed that the AlCl_3 could cause a shrinking of around 16% in the hippocampus pyramidal cells; besides, CoQ10 is a powerful therapeutic antioxidant to help restore the hippocampal neurons to a regular state.

Received 14th May 2021

Accepted 1st September 2021

DOI: 10.1039/d1ra03786b

rsc.li/rsc-advances

1. Introduction

Aluminum (Al) is a most plentiful metal; it can be found in water following its use in coagulation/flocculant agents during water purification.^{1–3} It can be found in food due to its use under acidic conditions as utensils and packaging for the food.⁴ Al can affect memory and cause risks in the mental growth of children.⁵ High levels of Al can induce neurodegenerative diseases such as Alzheimer's disease (AD) and Parkinson's disease.^{6,7} Some researchers supposed that the Al might pass through the blood–brain barrier and induce Alzheimer-like neurofibrillary tangles.^{8–11} It was suggested that the Al could generate free radicals that reduce the intracellular glutathione, damage the proteins and DNA, induce lipid peroxidation,¹² and cause

a decrease in the antioxidant enzyme state.¹³ Its compound, *i.e.*, aluminum chloride (AlCl_3), is considered a neurotoxin due to its ability to change both lipids and proteins.^{14,15} It can disturb and interfere with the acetylcholine metabolism and act as an etiopathogenic cofactor leading to neurodegenerative diseases.¹⁶ Many studies reported the ability of AlCl_3 to alter the membrane phospholipids' structure, function, and ion homeostasis.^{15,17} A daily dose of one g of AlCl_3 for ten days changed the molar ratio of cholesterol/phospholipid and induced membrane fluidity of cortex synaptosomes in the rat brain.¹⁸ Therefore, antioxidants that can minimize oxidative stress or stimulate the cellular antioxidants could protect against aluminum poisoning.¹⁹

Coenzyme Q10 (CoQ10) or vitamin Q10 (ref. 20) is a coenzyme Q family member that can be identified *via* the number of isoprenoid side-chains.²¹ In mitochondria, CoQ10 is the most common of this family. It is considered a cofactor in the mitochondrial electron-transport chain in which the redox reaction sequences are required to synthesize the adenosine triphosphate.²⁰ It is one of the most crucial antioxidants²² that reduces and prevents free radicals generation, and therefore, it can block the modifications and alteration of lipids, proteins, and DNA.²¹ Due to its ability to reduce the effects of oxidative stress, many research groups indicated that the administration of CoQ10 could treat the effects of neurological diseases, such as

^aDepartment of Physics, Faculty of Science, King Abdulaziz University, Jeddah 21589, Saudi Arabia. E-mail: Abdusaeed79@hotmail.com; Abdusaeed@tu.edu.ye; Tel: +966 563190832

^bDepartment of Physics, Thamar University, Thamar 87246, Yemen

^cBiochemistry Department, Faculty of Science, King Abdulaziz University, Jeddah, Saudi Arabia

^dKing Fahd Medical Research Center, Jeddah, Saudi Arabia

^eDepartment of Chemistry, College of Sciences, University of Ha'il, Ha'il 2440, Saudi Arabia

^fMedical Laboratories Department, Faculty of Applied Medical Sciences, Umm Al-Qura University, Mecca, Saudi Arabia



AD,²³ Parkinson's,²⁴ Huntington's,²⁵ amyotrophic lateral sclerosis,²⁶ and Friedreich's ataxia.²⁷

The hippocampus is considered a powerful part of the brain in vertebrates and humans. It plays a crucial role in reinforcing information between short-term memory and long-term memory. It is responsible for spatial memory that controls emotion and navigation,²⁸ modulates panic behaviors. Although the poisoning effects of AlCl_3 on the brain tissue and the protection of CoQ10 as antioxidants are well known; however, there are scarce studies that investigated the effects of AlCl_3 and CoQ10 on the lipids molecular structure and cells' morphological of the hippocampus brain tissue. Besides, to the best of our knowledge, this work is one of the first works investigating the cell diameter of brain hippocampus tissues under the effects of AlCl_3 and CoQ10. Fourier transform infrared (FTIR) spectroscopy and histopathology test were utilized to investigate the lipids' molecular structure and morphology of the hippocampal tissue cells, respectively. More details are in the following sections.

2. Experimental details

2.1. Animal and experimental design

From Animal House at King Fahd Medical Research Center (KFMRC), Wistar albino rats (twelve male) of 250 g and three months were utilized to perform the experiments. This study was performed according to the guidelines of the Declaration of Helsinki and approved by the Experimental Animal Research and Ethics Committee approved at KFMRC. The rats were randomly divided into three groups (4 rats per group). The first one was administered water; it was considered as the control group (C). The second one (A) was orally administered AlCl_3 (Sigma-Aldrich, Germany) dissolved in water (3 g L^{-1}) with a dose of 100 mg kg^{-1} for 4 weeks, according to the published report.²⁹ The last one (T) was orally administered AlCl_3 and treated at the same time by CoQ10 (Doctor's Best, USA) at a dose of 1200 mg kg^{-1} for 4 weeks; the dose of CoQ10 was reported by Li *et al.*³⁰ AlCl_3 and CoQ10 were used "as they are from the manufacturers" without further purification.

2.2. Samples' preparation

At the end of the duration, *i.e.*, 4 weeks, the rats were anesthetized; then, they were euthanized *via* decapitation. Every rat's whole brain was carefully and rapidly segregated from the skull. Then, the hippocampal tissues were isolated for performing FTIR spectroscopy, glutathione peroxidase (GPX) measurements, and histopathological study.

2.3. FTIR measurements

For FTIR measurements, the hippocampal tissues were immediately washed with normal saline; then, they were submerged within a tube in liquid nitrogen and kept at -80°C until use. They were lyophilized and gently grounded to be fine powder before recording their absorption FTIR spectra using Nicolet (iS10 FTIR) FTIR spectrometer (Thermo Scientific, USA) in the spectral region $4000\text{--}400 \text{ cm}^{-1}$ with an average of 40 scans and

spectral resolution of 4 cm^{-1} . Attenuated total reflection (ATR) was used as a sampling technique while recording the FTIR spectra. All FTIR spectra were recorded at room temperature and under identical conditions.

2.4. Measurement of GPX

GPX is an antioxidant enzyme in the cytosol and mitochondria; it reduces lipid peroxides (LOOH) and hydrogen peroxide (H_2O_2) to lipid alcohols and water, respectively, by catalyzing a redox reaction with reduced glutathione (GSH).³¹ GPX assay was performed using a GPX commercial enzyme-linked immunosorbent assay (ELISA) kit from MyBiosource, Inc. (San Diego, USA). In this protocol, a horseradish peroxidase (HRP) enzyme and sulphuric acid are used as the standard enzyme and stop solution, respectively; the color change is measured spectrophotometrically at 450 nm. According to the manufacturer's protocol, the hippocampus tissue homogenate was prepared, and the GPX measurements were performed. Briefly, $100 \mu\text{L}$ of the prepared hippocampus tissue homogenate was added to each well of the microtiter plate. Then, a $10 \mu\text{L}$ of balance solution and $50 \mu\text{L}$ of the conjugate were added to every well and mixed very well. The plate was then incubated for 1 hour at 37°C . After then, the wells were washed five times using a washing solution. After that, $50 \mu\text{L}$ substrate solutions were added to each well and incubated for 18 minutes at 37°C . Next, a $50 \mu\text{L}$ of stop solution was added to each well and mixed. Finally, the color (O.D.) intensity was determined at the wavelength of 450 nm using a microplate reader. The concentration of GPX for each sample was obtained by comparing its recorded O.D. with the standard curve.

2.5. Histopathological study

The extracted hippocampus tissues were placed in a vial containing 10% buffered formalin. After that, the tissues were embedded in paraffin. Then, each paraffin block was sectioned into 4–5 mm thick sections. Finally, the sections were stained with hematoxylin-eosin (H and E) to be examined *via* a light microscope.³²

2.6. Hippocampus cell morphology study

The histopathology images were used to estimate the average of the cells' diameters and their distribution analysis. After digitizing the histopathology images, the cells' diameters were calculated using ImageJ software (National Institute of Health, USA).

2.7. Statistical analysis

FTIR spectroscopy data were displayed using their average values \pm standard deviation of the mean (SD). The statistical significance was estimated using a *t*-test. The *p*-value < 0.05 was counted as a significant value. Multivariate analysis, *i.e.*, hierarchical cluster analysis (HCA) and principal components analysis (PCA), were performed to investigate the similarity between all tested rats' hippocampus brain tissues. These two



multivariate analyses can be applied to differentiate between the spectral data.^{33,34}

3. Results and discussion

3.1. FTIR spectroscopy

The recorded FTIR spectra for all rats' hippocampi tissues were baseline corrected; then, they were normalized according to the amide I band's absorbance.³⁵ The range of 3020–2840 cm^{-1} represents the lipids' characterization and contains the CH bands.^{36–41} The normalized absorbances (Norm. Abs.) of FTIR spectra for all tested rats in all groups in this range are displayed in Fig. 1a; the average spectra for every group are shown in Fig. 1b. As can be seen, all rats' FTIR spectra of the C group showed the highest intensity. In contrast, all rats' FTIR spectra of the A group showed the lowest intensity. In other words, in this region, all the A group bands decreased compared to those of the control group. At the same time, they increased in the T group compared to those of the A group. The CH bands are considered important indicators in this spectral range to determine whether the cell membrane's phospholipid structure is modified. Various information, such as the membrane ordering, saturation, fluidity, polarity, packing, and the hydrocarbon chain's length, can be extracted from these bands.

The most absorption bands in this spectral range are the olefinic=CH stretching band, $\nu_{\text{as}}(\text{CH}_3)$, $\nu_{\text{as}}(\text{CH}_2)$, $\nu_{\text{s}}(\text{CH}_3)$, and $\nu_{\text{s}}(\text{CH}_2)$ bands. Therefore, the CH band's spectral features, *i.e.*, center, full width at half maximum (FWHM), intensity, and

area, were estimated and tabulated in Tables 1 and 2. The beginning and ending points of CH bands during estimation of the spectral features are exhibited in Fig. 2. The average band centers for all groups are listed in Table 1, and they were assigned according to the published works.^{36–38} As can be noticed in Tables 1 and 2, significant changes were recorded in the bands center, FWHM, intensity, and area of olefinic=CH stretching, $\nu_{\text{as}}(\text{CH}_2)$, $\nu_{\text{s}}(\text{CH}_3)$, and $\nu_{\text{s}}(\text{CH}_2)$ bands ($p < 0.05$). The olefinic=CH stretching band shifted from $3014.01 \pm 0.05 \text{ cm}^{-1}$ in the C group to $3013.50 \pm 0.15 \text{ cm}^{-1}$ in the A group. The band's features of the olefinic=CH are generally used to monitor phospholipids' acyl chain saturation due to oxidative stress. It represents unsaturated lipids disordering resulting from the broken double bonds in the unsaturated acyl chains during lipid peroxidation.⁴² In the A group, the significant changes in the spectral features of the most intense $\nu_{\text{as}}(\text{CH}_2)$ band are considered a directrix for the disordered acyl chains and increased membrane fluidity⁴³ that could be referred to as the formation of soluble beta-amyloid (A β) around the nerve cells induced by Al;⁴⁴ A β can alter cell functions such as lipid transport,⁴⁵ and are involved in the pathogenesis of AD.^{46,47} At the same time, the significant changes in the $\nu_{\text{s}}(\text{CH}_3)$ and $\nu_{\text{s}}(\text{CH}_2)$ bands of the A group are indicators for the loss of acyl chain structure that happens during the *trans*-to-*gauche* transition.⁴⁸ The decrease in all CH bands' intensities (Table 2) in the A group could be referred to as the acyl chain composition's alterations. These results are expected, being that the AlCl₃ is a neurotoxin. Interestingly, in the $\nu_{\text{as}}(\text{CH}_2)$ and $\nu_{\text{s}}(\text{CH}_3)$ bands

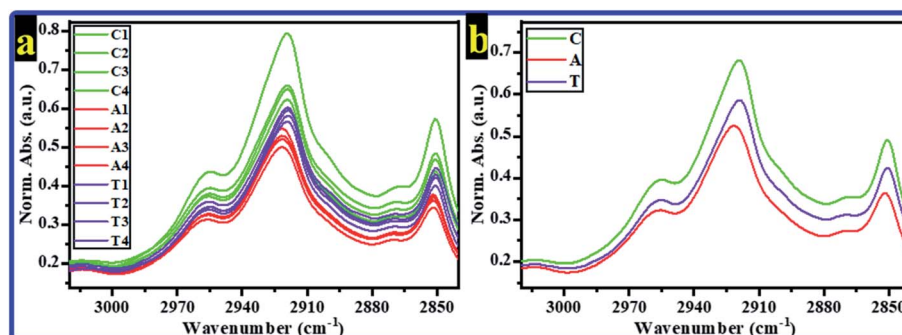


Fig. 1 Normalized absorbance of FTIR spectra of rats' brain hippocampal tissues for C, A, and T groups in the spectral region 3020–2840 cm^{-1} (a) all spectra of all rats, (b) average spectra.

Table 1 The bands' center^a and bands' FWHM^a of rats' hippocampus FTIR spectra in the spectral region of 3020–2840 cm^{-1} of C, A, and T groups^c

Band	Center (cm^{-1})			FWHM (cm^{-1})		
	C	A	T	C	A	T
Olefinic=CH	3014.01 ± 0.05	3013.50 ± 0.15^b	3014.20 ± 0.39	19.23 ± 0.87	21.01 ± 0.91^b	18.87 ± 0.74
$\nu_{\text{as}}(\text{CH}_3)$	2955.01 ± 0.63	2956.02 ± 0.04	2954.45 ± 0.43	46.07 ± 1.01	49.10 ± 0.97	48.23 ± 0.69
$\nu_{\text{as}}(\text{CH}_2)$	2919.02 ± 0.11	2922.05 ± 0.09^b	2919.01 ± 0.02	63.13 ± 0.99	66.53 ± 1.11^b	63.81 ± 1.59
$\nu_{\text{s}}(\text{CH}_3)$	2869.75 ± 0.39	2871.50 ± 0.45^b	2870.50 ± 0.51	12.75 ± 0.43	12.33 ± 0.56	12.50 ± 0.86
$\nu_{\text{s}}(\text{CH}_2)$	2850.75 ± 0.17	2851.69 ± 0.03^b	2850.19 ± 0.13	24.08 ± 0.63	25.50 ± 0.45^b	24.54 ± 0.39

^a Average values \pm SD. ^b Significant difference compared with the control values ($p < 0.05$). ^c v = stretch, as = antisymmetric, s = symmetric.



Table 2 The bands' intensity^a and bands' area^a of rats' hippocampus FTIR spectra in the spectral region of 3020–2840 cm^{−1} of C, A, and T groups

Band	Band intensity (a.u.)			Band area (a.u.)		
	C	A	T	C	A	T
Olefinic=CH	0.20 ± 0.00	0.19 ± 0.00 ^c	0.19 ± 0.00 ^b	4.06 ± 0.16	3.97 ± 0.05 ^b	3.76 ± 0.07
$\nu_{as}(CH_3)$	0.39 ± 0.02	0.32 ± 0.01 ^c	0.35 ± 0.01 ^b	14.53 ± 0.55	12.1 ± 0.18 ^b	13.13 ± 0.30
$\nu_{as}(CH_2)$	0.68 ± 0.07	0.52 ± 0.02 ^c	0.59 ± 0.01	33.43 ± 2.94	25.84 ± 0.69 ^c	28.95 ± 0.85 ^b
$\nu_s(CH_3)$	0.35 ± 0.03	0.27 ± 0.01 ^c	0.31 ± 0.01	4.78 ± 0.23	3.57 ± 0.21 ^b	4.15 ± 0.15
$\nu_s(CH_2)$	0.49 ± 0.05	0.36 ± 0.01 ^c	0.42 ± 0.02 ^b	10.00 ± 0.91	8.01 ± 0.17 ^c	9.02 ± 0.51 ^b

^a Average values ± SD. ^b Significant difference compared with the control values ($p < 0.05$). ^c Significant difference compared with the control values ($p < 0.01$).

intensity, no significant changes were detected in the T group compared to the C group, indicating the antioxidant action of CoQ10 in the T group. In olefinic=CH stretching, $\nu_{as}(CH_3)$, $\nu_{as}(CH_2)$, $\nu_s(CH_3)$ and $\nu_s(CH_2)$ bands' intensity, decreases were observed in the treated group; however, they were not similar to the decreases in the administered $AlCl_3$ group.

FTIR spectra' CH bands intensity ratios for rats' brain hippocampal tissues were evaluated to explore the lipid profile. The intensity ratios olefinic=CH/ $\nu_{as}(CH_3)$, $\nu_{as}(CH_2)/\nu_{as}(CH_3)$, and $\nu_{as}(CH_2)/[\nu_{as}(CH_2) + \nu_s(CH_2)]$ were used as indicators for the unsaturated level of phospholipids, lipid acyl chain unsaturation, and phospholipids chain length, respectively.^{36–38,49,50} The average evaluated band intensity ratios with their SD are listed in Table 3. The noticeable increase in the olefinic=CH/ $\nu_{as}(CH_3)$ ratio for the rats of the A group compared to the rats of the C group could be referred to as the unsaturated to saturated lipids increase in the cell membrane of the hippocampal tissues intercede by the toxicity of $AlCl_3$ where fatty acids degrade to the shorter chain happens by oxidative stress induced by $AlCl_3$, suggesting the end products of lipid peroxidation accumulate.⁴⁹ Although there is a significant increase in olefinic=CH/ $\nu_{as}(CH_3)$ ratio for the T ($AlCl_3/CoQ10$) group compared to the control group; however, the ratio is still less than those of the A group ratio, suggesting the CoQ10 was able to minimize the effect of $AlCl_3$ toxicity. Simultaneously, the decrease in the

$\nu_{as}(CH_2)/\nu_{as}(CH_3)$ intensity ratio in hippocampus brain tissue in the $AlCl_3$ group is also an allusion of higher polarity and lipid acyl chain unsaturation, suggesting lipid acyl chain peroxidation.⁵¹ The intensity ratio of $\nu_{as}(CH_2)/[\nu_{as}(CH_2) + \nu_s(CH_2)]$ was used to hydrocarbon chain length. A significant increase was detected in this ratio in the A group, suggesting an increase in the phospholipids chain length. No considerable changes were recorded between the C and T groups, indicating the effect of CoQ10 as an antioxidant factor.

Multivariate analyses, *i.e.*, HCA and PCA were carried out to study the similarity between the FTIR spectra of rats' brain hippocampal tissues in the spectral region of 3020–2840 cm^{−1}. The Norm. Abs. of FTIR spectra were used to perform the HCA and PCA, and the results are shown in Fig. 3a and 4b, respectively. Unfortunately, the HCA and PCA failed to differentiate between all rats' FTIR spectra completely. Therefore, the second derivative (2nd der.) was applied in all FTIR spectra; the second derivative is a spectroscopy method to boost the segregation of overlapping bands.⁵²

The 2nd der. for all FTIR spectra of rats' brain hippocampal tissues from all groups are shown in Fig. 4a. Simultaneously, the averages of 2nd der. for every group are illustrated in Fig. 4b. The 2nd der. displays clearly the differences in the bands' shift and intensity between groups. Then, the HCA and PCA were re-performed in the 2nd der. data of FTIR, their results are displayed in Fig. 4c and d, respectively. The HCA successfully recognizes every group; interestingly, the rats of the C and T groups were included in one branch. However, the A group's rats were included in the other branch. These results mean the rats' brain hippocampal tissues from the control and $AlCl_3/CoQ10$ groups have the same similarity. At the same time, they are different from those of the $AlCl_3$ group. The PCA results (Fig. 4d) confirmed the HCA results where the rats of both the C and T groups distributed on the negative side of PC1; simultaneously, the T group rats distributed on the positive side of PC1. PC1 and PC2 recorded 85.38% and 10.46% of the total variance, respectively.

From FTIR results and as mentioned previously, Al can induce the formation of A β , which is associated with AD pathogenesis. A β has the ability to enter the membrane and change the phospholipids' structure and function; it can produce free radicals, causing lipid peroxidation and modulating ion channels.⁵³ However, in the group administered by $AlCl_3/CoQ10$, no

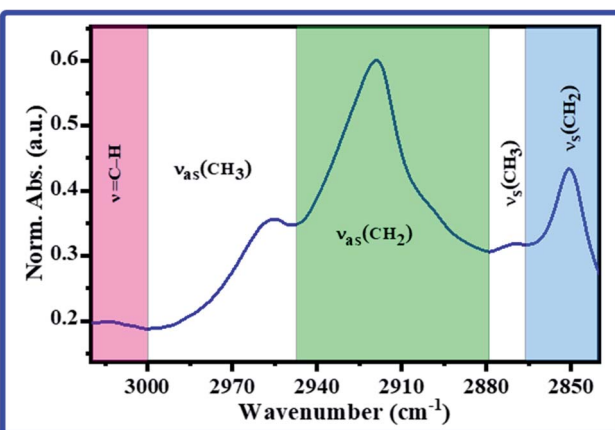


Fig. 2 The beginning and end of the lipid bands for estimation of the bands' area and FWHM in the FTIR spectrum of rats' hippocampus.



Table 3 The bands' intensity^a ratio of rats' hippocampus FTIR spectra in the spectral region of 3020–2840 cm^{−1} of C, A, and T groups

Band	Intensity ratio		
	C	A	T
Olefinic=CH/ $\nu_{as}(CH_3)$	0.514 ± 0.091	0.580 ± 0.062 ^b	0.559 ± 0.101 ^b
$\nu_{as}(CH_2)/\nu_{as}(CH_3)$	1.719 ± 0.095	1.623 ± 0.083 ^b	1.688 ± 0.075
$\nu_{as}(CH_2)/[\nu_{as}(CH_2) + \nu_s(CH_2)]$	0.581 ± 0.019	0.590 ± 0.026 ^b	0.580 ± 0.033

^a Average values ± SD. ^b Significant difference compared with the control values ($p < 0.05$).

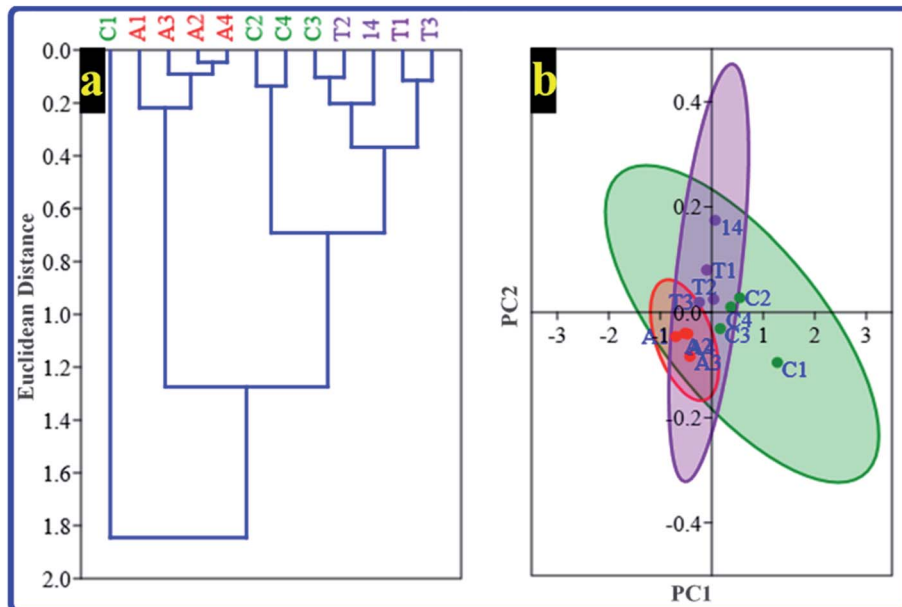


Fig. 3 Multivariate analysis extracted from Norm. Abs. of FTIR spectra for all rats' hippocampus brain tissue for C, A, and T groups in the region 3020–2840 cm^{−1} that includes the lipid's features (a) HCA and (b) PCA.

significant changes were noticed in the lipid structure compared with the control group, indicating the antioxidation effect of CoQ10, which could discourage, reduce, and cancel the effect and the toxicity of the AlCl₃.

3.2. GPX

The GPX results revealed a significant decrease in the GPX value of the A group by comparing it with the value of the C group. In contrast, no significant changes can be detected between the C and T groups (Fig. 5). These results indicate a decrease in the activity of the GPX of rats by administered AlCl₃ compared with the control group; simultaneously, the rats treated by CoQ10 showed GPX activity similar to the control rats. The lower activity of the GPX enzyme could be illustrated by the consumption of the antioxidant protection system to overcome the overgeneration of free radicals,^{54,55} which AlCl₃ could produce. Besides, the GPX enzyme is a relatively stable enzyme during normal conditions, while it could be inactivated in acute oxidative stress conditions⁵⁵ that result from AlCl₃. Furthermore, reactive oxygen species (ROS) overproduction reduces the endogenous antioxidant system, causing damage to the cells due to oxidative stress. While, in group T that AlCl₃ and CoQ10

were administered, the CoQ10 could cancel and overcome the effects of the AlCl₃; it could enhance the antioxidant system, leading to a decrease in ROS production.

3.3. Histological test

The histological test is a good choice for studying the hippocampus as the most brain region in jeopardy for AD. In the present study, histological test results of rats' hippocampal tissues are exhibited in Fig. 6. The histopathology images of the C, A, and T groups can be seen in Fig. 6a–c, respectively. The images showed small pyramidal cells with vesicular nuclei in all tested samples. The histology images revealed that no detectable differences could be notified between the control and AlCl₃/CoQ10 groups. However, the images uncovered two different features between the C and A groups. The first feature showed alteration in pyramidal cells' shape, where they seemed to be more circular in the A group. The second feature can be detected in the shrinking of pyramidal cells in rats administered AlCl₃. The shrinking in the pyramidal cells was investigated by exploring their diameters. Fig. 6d–f exhibited the cell diameters distribution histograms for the C, A, and T groups, respectively. The rats administered AlCl₃ showed statistically



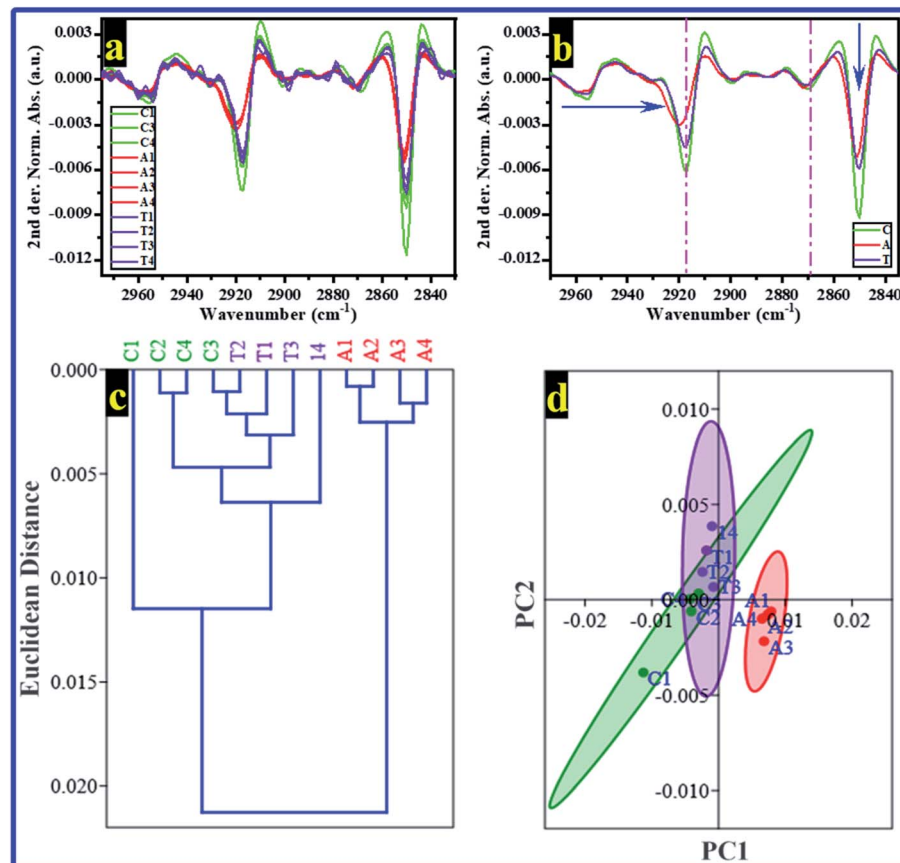


Fig. 4 The 2nd der. Norm. Abs. of FTIR spectra between 3020 and 2840 cm^{-1} and their extracted multivariate analysis for rats' hippocampus brain tissue obtained from C, A, and T groups (a) 2nd der. Norm. Abs. of FTIR spectra for all rats, (b) the average of the 2nd der. Norm. Abs. for every group, (c) HCA, and (d) PCA.

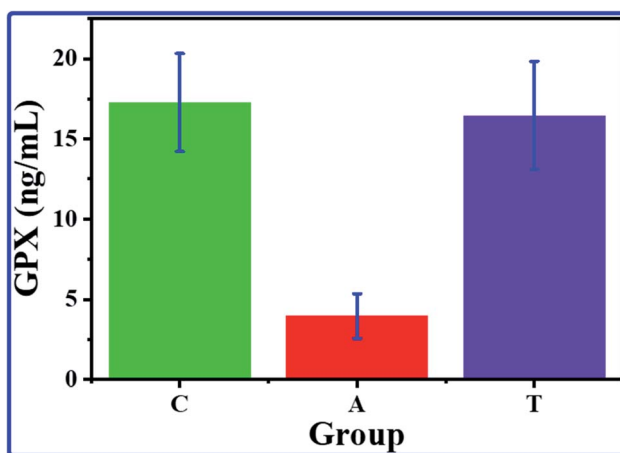


Fig. 5 The average GPX concentrations with their SD for hippocampus brain tissue of C, A, and T groups.

significant decreases in their cell diameters compared with the control group, where the estimated cell sizes were found to be $4.81 \pm 0.55 \mu\text{m}$, $4.04 \pm 0.71 \mu\text{m}$, and $4.63 \pm 0.71 \mu\text{m}$ for the C, A, and T groups, respectively. These signs were perceived in the

hippocampus' neuron with loss of some cell;⁵⁶ it was proven that the AlCl_3 administration could cause the outcrop of neurotic plaques in the hippocampal tissues with a black center.¹⁵ These observations are typical for AD disease; besides, they were observed in the rats' hippocampus brain tissues receiving only AlCl_3 . These indicators are considered clear evidence of oxidative damage and chronic inflammation. These observations are due to the AlCl_3 could stimulate degenerative neuronal alterations in hippocampal neurons similar to those reported in the published work.¹⁵

Fig. 7 explains and summarizes the histopathology results of the brain tissue hippocampal cells extracted and stained from C, A, T groups. The figure shows that the pyramidal cells of those rats administered by AlCl_3 shrunk and dark center dots compared to the control rats. However, there are no considerable differences between the C and T groups. $\text{AlCl}_3/\text{CoQ10}$ administration demonstrated a better histological picture, meaning the CoQ10 can be used as an antioxidant protective agent. CoQ10 could be an operative curative substance as it rejuvenates the hippocampal neurons to regular status. Therefore, coenzyme Q10 has a powerful antioxidant capacity, reduces oxidative stress, counteracts oxidative damage, and protects from brain neurodegeneration caused by AlCl_3 .

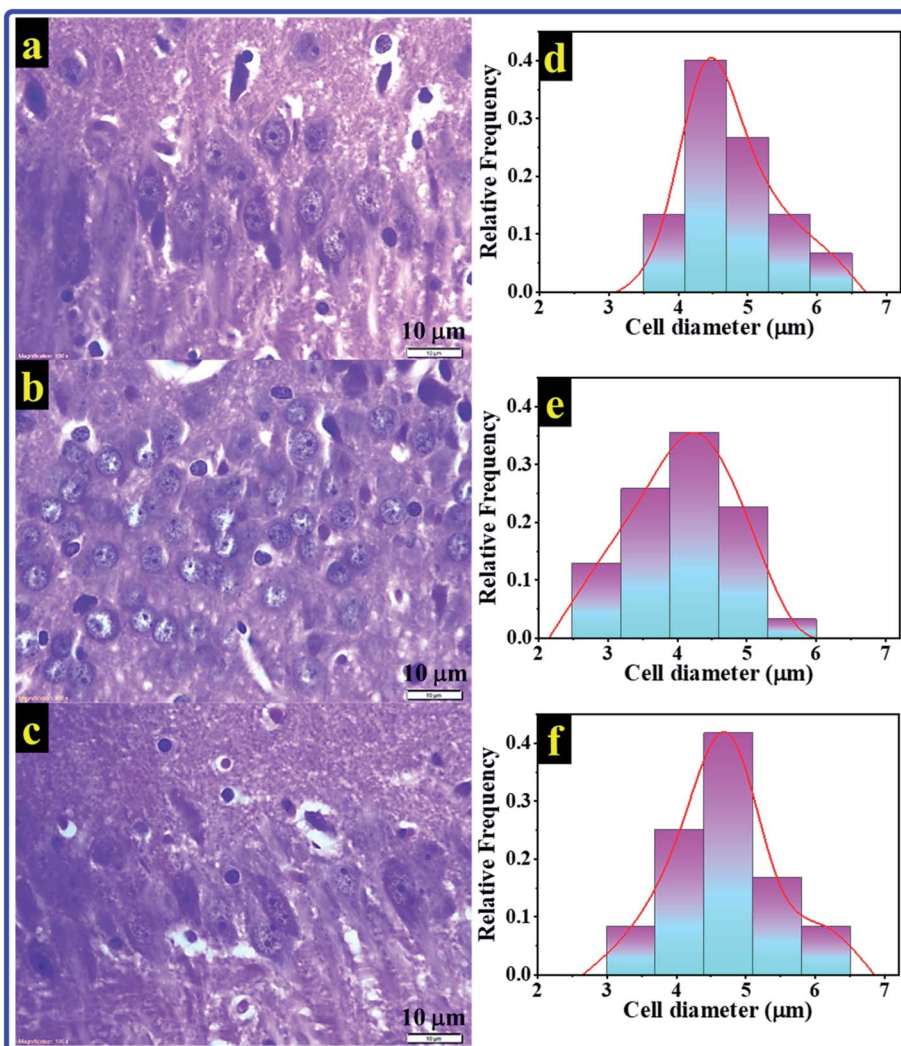


Fig. 6 H&E stained histopathology images for sections of the hippocampus of (a) C, (b) A, and (c) T groups. The estimated pyramidal cells' diameter with their distribution of (d) C, (e) A, and (f) T groups.

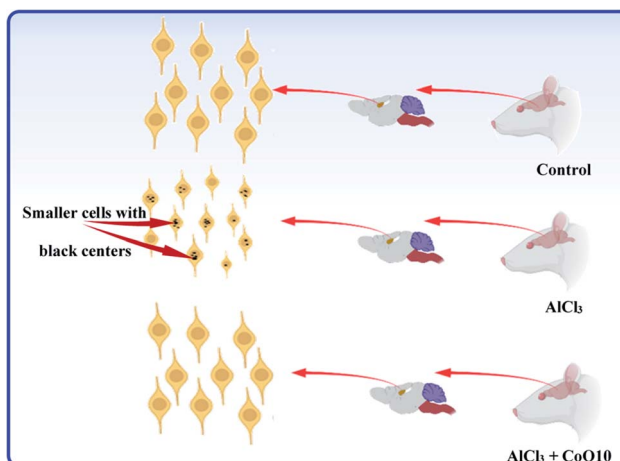


Fig. 7 The schematic graph illustrates the effects of AlCl₃ and CoQ10 in the hippocampus's pyramidal cells.

4. Conclusion

The effects of AlCl₃ and CoQ10 on the brain hippocampal tissue's lipid molecular structure and cells' morphology have been investigated in this work. AlCl₃ and CoQ10 were explored as neurotoxin and antioxidant materials, respectively. FTIR results showed changes in the lipids' molecular in the rats take AlCl₃ in their drink water; simultaneously, no changes were detected in those rats take AlCl₃ and CoQ10 simultaneously. Histopathology results also showed alterations in the hippocampal tissue's pyramidal cells' sizes, where they were shrinking by around 16% in the rats that take AlCl₃. In contrast, no significant changes in the pyramidal cells were observed in those rats take AlCl₃ and CoQ10. This study's finding is that CoQ10 is a powerful therapeutic antioxidant to maintain the molecular structure of lipids and the morphology of hippocampal cells; despite the toxicity of AlCl₃, CoQ10 can help restore neurons in the hippocampus to a normal state.

Author contributions

A. S. (Abdu Saeed): conceptualization, software, data curation, writing – review & editing. S. Y. Q. (Safaa Y. Qusti): conceptualization, supervision, writing – review & editing. R. H. A. (Rawan Hamdan Almarwani): methodology, investigation, experiment measurements, writing – original draft. E. J. J. (Ebtihaj J. Jambi): validation, writing – review & editing. E. M. A. (Eida M. Alshammari): validation, writing – review & editing. N. F. G (Naeem F. Gusty): validation, writing – review & editing. M. J. B. (Maha J. Balgoon): conceptualization, supervision, writing – review & editing.

Conflicts of interest

The authors declare no conflict of interest.

References

- Z. Wu, X. Zhang, J. Pang, J. Li, J. Li and P. Zhang, *RSC Adv.*, 2020, **10**, 7155–7162.
- H. Cui, X. Huang, Z. Yu, P. Chen and X. Cao, *RSC Adv.*, 2020, **10**, 20231–20244.
- S. Zhao, F. Wang, W. Jia, Q. Sun and Z. Zou, *RSC Adv.*, 2019, **9**, 40316–40325.
- T. Stahl, S. Falk, A. Rohrbeck, S. Georgii, C. Herzog, A. Wiegand, S. Hotz, B. Boschek, H. Zorn and H. Brunn, *Environ. Sci. Eur.*, 2017, **29**, 17.
- W. Zhong, L. Wang, S. Fang, D. Qin, J. Zhou, G. Yang and H. Duan, *RSC Adv.*, 2020, **10**, 3048–3059.
- E. Inan-Eroglu and A. Ayaz, *J. Res. Med. Sci.*, 2018, **23**, 51.
- S. Maya, T. Prakash, K. D. Madhu and D. Goli, *Biomed. Pharmacother.*, 2016, **83**, 746–754.
- J. R. McDermott, A. I. Smith, K. Iqbal and M. D. H. M. Wisniewski, *Neurology*, 1979, **29**, 809.
- R. Anane, M. Bonini, J. M. Geraud and E. E. Creppy, *Arch. Toxicol.*, 1995, **69**, 568–571.
- R. Deloncle and O. Guillard, *Neurochem. Res.*, 1990, **15**, 1239–1245.
- D. Sharma, P. Sethi, E. Hussain and R. Singh, *Biogerontology*, 2009, **10**, 489–502.
- M. A. González, C. A. Bernal, S. Mahieu and M. C. Carrillo, *Biol. Trace Elem. Res.*, 2008, **127**, 164.
- C. Swain and G. B. N. Chainy, *Mol. Cell. Biochem.*, 1998, **187**, 163–172.
- A. A. Shati, F. G. Elsaid and E. E. Hafez, *Neuroscience*, 2011, **175**, 66–74.
- M. J. Balgoon, G. A. R. Ahmed, S. Y. Qusti and S. Shaker, *Neurol. Psychiatr. Brain Res.*, 2019, **31**, 1–8.
- P. Zatta, M. Ibn-Lkhayat-Idrissi, P. Zambenedetti, M. Kilyen and T. Kiss, *Brain Res. Bull.*, 2002, **59**, 41–45.
- G. A. R. Ahmed, W. El Hotaby, L. Abbas, H. H. A. Sherif, G. Kamel and S. K. H. Khalil, *Spectrochim. Acta, Part A*, 2020, **239**, 118421.
- V. S. Silva, J. Miguel Cordeiro, M. J. Matos, C. R. Oliveira and P. P. Gonçalves, *Neurosci. Res.*, 2002, **44**, 181–193.
- A. E. Abdel Moneim, *Biol. Trace Elem. Res.*, 2012, **150**, 328–336.
- R. Saini, *J. Pharm. BioAllied Sci.*, 2011, **3**, 466–467.
- M. Spindler, M. F. Beal and C. Henchcliffe, *Neuropsychiatr. Dis. Treat.*, 2009, **5**, 597–610.
- Y. Wang, S. Chen, J. Liu, P. Lv, D. Cai and G. Zhao, *RSC Adv.*, 2019, **9**, 22336–22342.
- X. Yang, Y. Yang, G. Li, J. Wang and E. S. Yang, *J. Mol. Neurosci.*, 2008, **34**, 165–171.
- C. W. Shults, M. Flint Beal, D. Song and D. Fontaine, *Exp. Neurol.*, 2004, **188**, 491–494.
- W. J. Koroshetz, B. G. Jenkins, B. R. Rosen and M. F. Beal, *Ann. Neurol.*, 1997, **41**, 160–165.
- P. Kaufmann, J. L. P. Thompson, G. Levy, R. Buchsbaum, J. Shefner, L. S. Krivickas, J. Katz, Y. Rollins, R. J. Barohn, C. E. Jackson, E. Tiryaki, C. Lomen-Hoerth, C. Armon, R. Tandan, S. A. Rudnicki, K. Rezania, R. Sufit, A. Pestronk, S. P. Novella, T. Heiman-Patterson, E. J. Kasarskis, E. P. Pioro, J. Montes, R. Arbing, D. Vecchio, A. Barsdorf, H. Mitsumoto, B. Levin and Q. S. Group, *Ann. Neurol.*, 2009, **66**, 235–244.
- J. M. Cooper, L. V. Korlipara, P. E. Hart, J. L. Bradley and A. H. Schapira, *Eur. J. Neurol.*, 2008, **15**, 1371–1379.
- A. R. Preston and H. Eichenbaum, *Curr. Biol.*, 2013, **23**, R764–R773.
- G.-f. Zeng, Z.-y. Zhang, L. Lu, D.-q. Xiao, S.-h. Zong and J.-m. He, *Rejuvenation Res.*, 2013, **16**, 124–133.
- G. Li, L. Zou, C. R. Jack, Y. Yang and E. S. Yang, *Neurobiol. Aging*, 2007, **28**, 877–882.
- M. Higuchi, in *Wheat and Rice in Disease Prevention and Health*, ed. R. R. Watson, V. R. Preedy and S. Zibadi, Academic Press, San Diego, 2014, pp. 181–199, DOI: 10.1016/b978-0-12-401716-0.00015-5.
- J. D. Bancroft and M. Gamble, *Theory and practice of histological techniques*, Elsevier Health Sciences, 2008.
- M. A. N. Razvi, A. Bakry, A. Saeed, S. M. Afzal, Y. F. AL-Hadeethi, J. AL-Maghribi and S. AL-Muhayawi, *Sci. Adv. Mater.*, 2020, **12**, 853–860.
- A. Saeed and F. Abolaban, *Spectrochim. Acta, Part A*, 2021, **261**, 120082.
- S. S. Nafee, A. Saeed, S. A. Shaheen, S. M. El Assouli, M. Z. E. Assouli and G. A. Raouf, *Health Phys.*, 2016, **110**, 50–58.
- A. Saeed, M. N. Murshed and E. A. Al-Shahari, *Environ. Sci. Pollut. Res.*, 2020, **27**, 40443–40455.
- A. Saeed, G. A. Raouf, S. S. Nafee, S. A. Shaheen and Y. Al-Hadeethi, *PLoS One*, 2015, **10**, e0139854.
- A. Saeed and F. Abolaban, *Biochem. Biophys. Res. Commun.*, 2020, **533**, 1048–1053.
- I. de la Arada, E. J. González-Ramírez, A. Alonso, F. M. Goñi and J.-L. R. Arondo, *Sci. Rep.*, 2020, **10**, 17606.
- A. Prasad, A. Chaichi, D. P. Kelley, J. Francis and M. R. Gartia, *RSC Adv.*, 2019, **9**, 24568–24594.
- N. S. Elkholly, M. W. Shafaa and H. S. Mohammed, *RSC Adv.*, 2020, **10**, 32409–32422.
- F. Severcan, N. Kaptan and B. Turan, *Spectroscopy*, 2003, **17**, 472834.



43 H. L. Casal and H. H. Mantsch, *Biochim. Biophys. Acta, Rev. Biomembr.*, 1984, **779**, 381–401.

44 G. A.-R. Ahmed, S. K. H. Khalil, W. El hotaby, L. Abbas, H. H. A. Sherif, E. A. Abdel-Rahman, S. H. Saber, M. Hassan, M. H. Hassan and S. S. Ali, *Spectrochim. Acta, Part A*, 2020, **228**, 117535.

45 M. J. Balgoon, G. A. Raouf, S. Y. Qusti and S. S. Ali, *Int. J. Med. Health Biomed. Bioeng. Pharm. Eng.*, 2015, **9**, 782–792.

46 H. Ahyayauch, A. B. García-Arribas, M. E. Masserini, S. Pantano, F. M. Goñi and A. Alonso, *Int. J. Biol. Macromol.*, 2020, **164**, 2651–2658.

47 H. Ahyayauch, M. Masserini, F. M. Goñi and A. Alonso, *Int. J. Biol. Macromol.*, 2021, **168**, 611–619.

48 F. Ripanti, A. Di Venere, M. Cestelli Guidi, M. Romani, A. Filabozzi, M. Carbonaro, M. C. Piro, F. Sinibaldi, A. Nucara and G. Mei, *Int. J. Mol. Sci.*, 2021, **22**, 1334.

49 G. Cakmak, L. M. Miller, F. Zorlu and F. Severcan, *Arch. Biochem. Biophys.*, 2012, **520**, 67–73.

50 A. Rodríguez-Casado, I. Alvarez, A. Toledano, E. de Miguel and P. Carmona, *Biopolymers*, 2007, **86**, 437–446.

51 C. Petibois, G. Cazorla, J.-R. Poortmans and G. Délérés, *Sports Med.*, 2003, **33**, 83–94.

52 L. Rieppo, S. Saarakkala, T. Närhi, H. J. Helminen, J. S. Jurvelin and J. Rieppo, *Osteoarthritis Cartilage*, 2012, **20**, 451–459.

53 M. Kawahara and M. Kato-Negishi, *Int. J. Alzheimer's Dis.*, 2011, **2011**, 276393.

54 A. K. Singh, P. Pandey, M. Tewari, H. P. Pandey, I. S. Gambhir and H. S. Shukla, *J. Postgrad. Med.*, 2016, **62**, 96–101.

55 J. Dworzański, M. Strycharz-Dudziak, E. Kliszczewska, M. Kiełczykowska, A. Dworzańska, B. Drop and M. Polz-Dacewicz, *PLoS One*, 2020, **15**, e0230374.

56 F. M. Ghoneim, H. A. Khalaf, A. Z. Elsamanoudy, S. M. Abo El-Khair, A. M. N. Helaly, E.-H. M. Mahmoud and S. H. Elshafey, *Int. J. Clin. Exp. Pathol.*, 2015, **8**, 7710–7728.

